

Original article

4-Nitroacetophenone-derived thiosemicarbazones and their copper(II) complexes with significant *in vitro* anti-trypanosomal activity

Anayive Pérez-Rebolledo^a, Leticia R. Teixeira^b, Alzir A. Batista^c, Antonio S. Mangrich^d, Gabriela Aguirre^e, Hugo Cerecetto^e, Mercedes González^e, Paola Hernández^e, Ana M. Ferreira^f, Nivaldo L. Speziali^g, Heloisa Beraldo^{a,*}

^a Departamento de Química, Universidade Federal de Minas Gerais, 31270-901 Belo Horizonte, MG, Brazil

^b Departamento de Química, Pontifícia Universidade Católica do Rio de Janeiro, 22453-900 Rio de Janeiro, Brazil

^c Departamento de Química, Universidade Federal de São Carlos, 1365-905 São Carlos, Brazil

^d Departamento de Química, Universidade Federal do Paraná, 81.531-990 Curitiba, Brazil

^e Departamento de Química Orgánica, Universidad de la República, 11400 Montevideo, Uruguay

^f Cátedra de Inmunología, Universidad de la República, 11600 Montevideo, Uruguay

^g Departamento de Física, Universidade Federal de Minas Gerais, 31270-901 Belo Horizonte, MG, Brazil

Received 26 April 2007; received in revised form 20 June 2007; accepted 22 June 2007

Available online 10 July 2007

Abstract

*N*⁴-Methyl-4-nitroacetophenone thiosemicarbazone (H4NO₂Ac4M, **1**), *N*⁴,*N*⁴-dimethyl-4-nitroacetophenone thiosemicarbazone (H4NO₂Ac4DM, **2**) and *N*⁴-piperidyl-4-nitroacetophenone thiosemicarbazone (H4NO₂Ac4Pip, **3**) and their copper(II) complexes [Cu(4NO₂Ac4M)₂] (**4**), [Cu(4NO₂Ac4DM)₂] (**5**) and [Cu(4NO₂Ac4Pip)₂] (**6**) were tested for their *in vitro* ability to inhibit the growth of *Trypanosoma cruzi* epimastigote forms. H4NO₂Ac4DM (**2**), [Cu(4NO₂Ac4M)₂] (**4**) and [Cu(4NO₂Ac4DM)₂] (**5**) proved to be as active as the clinical reference drugs nifurtimox and benznidazol. Taking into consideration the serious side effects and the poor efficacy of the reference drugs, as well as the appearance of resistance during treatment, the studied compounds could constitute a new class of anti-trypanosomal drug candidates.

© 2007 Elsevier Masson SAS. All rights reserved.

Keywords: 4-Nitroacetophenone thiosemicarbazones; Copper(II) complexes; Anti-trypanosomal activity

1. Introduction

Parasitic diseases affect hundreds of millions of people around the world, mainly in underdeveloped countries. Since parasitic protozoa are eukaryotic they share many common features with their mammalian hosts making the development of effective and selective drugs a hard task. Despite the great effort that has been made in the discovery of unique targets that afford selectivity, many of the drugs used today have serious side effects. Diseases caused by *Trypanosomatidae*, which share a similar state regarding drug treatment, include Chagas' disease, caused by *Trypanosoma cruzi*. *T. cruzi* alone

is responsible for an infected population of nearly 20 millions and more than 200 millions are at risk [1,2].

Current treatment of the disease has been based on nifurtimox (nfx, 4-[(5-nitrofurfurylidene)-amino]-3-methylthio morpholine-1,1-dioxide), a nitrofurane derivative produced only in El Salvador by Bayer, and benznidazole (bnz, *N*-benzyl-2-nitro-1-imidazoleacetamide), a nitroimidazole derivative produced by Roche (see Fig. 1a). They were introduced empirically over three decades ago. Both drugs are active in the acute phase of the disease but their efficacies are very low in the established chronic phase. These compounds cause serious undesirable side effects and show poor clinical efficacy [2].

Both drugs act via reduction of the nitro group. In the case of nfx, reduction generates an unstable nitro anion radical, which produces highly toxic reduced oxygen species

* Corresponding author. Tel.: +55 31 3499 5740; fax: +55 31 3499 5700.

E-mail address: hberaldo@ufmg.br (H. Beraldo).

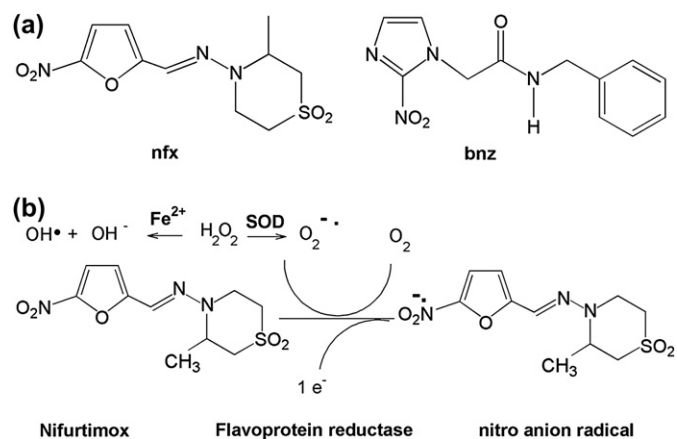


Fig. 1. (a) Chemical structures of nifurtimox (nfx, 4-[(5-nitrofurfurylidene)-amino]-3-methylthio morpholine-1,1-dioxide) and benznidazole (bnz, *N*-benzyl-2-nitro-1-imidazoleacetamide); (b) proposed mechanism of action of nfx.

(Fig. 1b), whereas the mechanism of action of bnz involves covalent modification of macromolecules by nitro reduction intermediates [3].

Thiosemicarbazones, semicarbazones and their metal complexes represent an interesting class of compounds with a wide range of pharmacological applications [4]. However, few works deal with nitro derivatives. Recently, the literature has described that some semicarbazones and thiosemicarbazones exhibit trypanocidal activity against parasites in cell culture. Hence 5-nitro-2-furaldehyde and 5-nitrothiophene-2-carboxaldehyde semicarbazone derivatives and 5-nitrofuryl-containing thiosemicarbazones were found to be active against *T. cruzi* [2,5,6].

It has been shown that some metal complexes of anti-trypanosomal drugs resulted to be more active than the corresponding free ligands [7,8], suggesting that the preparation of metal complexes with ligands bearing anti-trypanosomal activity could be a successful strategy for the development of new anti-Chagas' disease agents. As a first stage, palladium and platinum have been selected as central metals because of the postulated metabolic similarities between tumor cells and *T. cruzi* cells [9]. On the other hand some copper compounds have shown the ability to bind DNA as the main mechanism of anti-tumoral action [10]. In addition, copper complexes have shown activity as anti-parasites against *Entamoeba histolytica*, and as anti-microbials against *Mycobacterium tuberculosis*, acting through different mechanisms [11].

To our knowledge the anti-trypanosomal activity of nitroacetophenone thiosemicarbazones has not been investigated. In most cases *N*(4)-alkyl or *N*(4)-aryl thiosemicarbazones exhibit higher pharmacological activity in comparison to their unsubstituted analogues, probably due to increased lipophilicity [4]. Therefore, in the present work *N*⁴-methyl- (H4NO₂Ac4M, **1**), *N*⁴,*N*⁴-dimethyl- (H4NO₂Ac4DM, **2**) and *N*⁴-piperidyl-4-nitroacetophenone thiosemicarbazone (H4NO₂Ac4Pip, **3**) (Fig. 2) and their copper(II) complexes were prepared and tested for their *in vitro* ability to inhibit the growth of *T. cruzi* epimastigote forms.

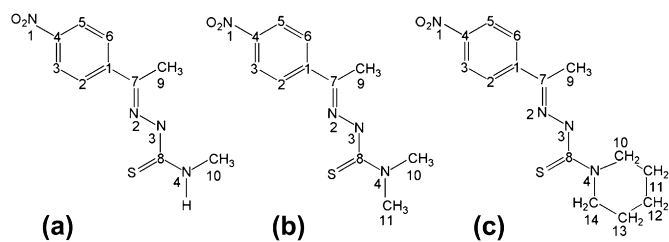


Fig. 2. Chemical structures of 4-nitroacetophenone thiosemicarbazones, showing the numbering system used: (a) H4NO₂Ac4M (**1**), (b) H4NO₂Ac4DM (**2**) and (c) H4NO₂Ac4Pip (**3**).

2. Results and discussion

2.1. NMR studies of H4NO₂Ac4M (**1**), H4NO₂Ac4DM (**2**) and H4NO₂Ac4Pip (**3**)

The ¹H resonances were assigned on the basis of chemical shifts, multiplicities and coupling constants. The carbon type (C, CH) was determined by using DEPT 135 experiments.

The NMR spectra of **1** were studied previously [12]. In the ¹H NMR (DMSO-*d*₆) spectrum of the thiosemicarbazones the signal of N(3)–H is found in the δ 10.46–9.84 range. This high frequency signal is due to hydrogen bonding with the solvent [12,13]. In the spectra of **2** and **3** one doublet attributed to H(3,5) was observed at δ 8.29 and δ 8.25, respectively, and a second doublet attributed to H(2,6) was found at δ 8.05 and δ 8.01, respectively, resulting from the vicinal coupling of H(2) with H(3) and of H(5) with H(6). In the spectrum of **1** only one sharp singlet had been observed for the aromatic hydrogens at δ 8.20, indicating equivalency of the four hydrogens. In the ¹³C NMR spectrum only small differences were observed in the chemical shifts of C=N and C=S for the three thiosemicarbazones (see Section 4.3).

2.2. Microanalyses, molar conductivity and magnetic susceptibility studies of the copper(II) complexes

Microanalyses and molar conductivity data suggest the formation of [Cu(4NO₂Ac4M)₂] (**4**), [Cu(4NO₂Ac4DM)₂] (**5**) and [Cu(4NO₂Ac4Pip)₂] (**6**). The effective magnetic moments in the 1.50–1.80 BM range are compatible with the theoretical spin only value of 1.73 BM for copper(II) complexes.

2.3. Infrared and electronic spectral studies

In the infrared spectra, the ν (C=N) stretching vibration of the thiosemicarbazones at 1590 cm⁻¹ shifts to 1585–1568 cm⁻¹ in the complexes, indicating coordination of the imine nitrogen [14–16]. The absorption at 818–806 cm⁻¹ in the spectra of the free bases, attributed to the ν (C=S) vibration, shifts to 751–719 cm⁻¹ in the spectra of the complexes, indicating complexation through a thiolate sulfur [17]. Absorptions at 452–432 cm⁻¹ and 368–322 cm⁻¹ in the spectra of the complexes were attributed to the ν (Cu–N) and ν (Cu–S) vibrations [18]. Hence the infrared spectra indicate coordination through the N–S chelating system.

The $n-\pi^*$ transitions at 27,951–27,225 cm^{-1} attributed to the azomethine and thioamide functions in the electronic spectra of the thiosemicarbazones [19], overlap in the 29,939–29,561 cm^{-1} range in the spectra of the complexes. The $N-\text{Cu}^{\text{II}}$ and $S-\text{Cu}^{\text{II}}$ ligand-to-metal charge transfer transitions were found at 25,060–24,312 cm^{-1} and the ligand field transitions at 17,126–16,664 cm^{-1} [20].

2.4. EPR spectra of the copper(II) complexes

The X-band EPR spectra of frozen solutions of complexes **4**, **5** and **6** in DMF are shown in Fig. 3. The Hamiltonian parameters are resumed in Table 1.

The EPR spectra of the three complexes indicate axial symmetry. For all compounds $g_{\parallel} > g_{\perp} > 2$, in accordance with approximately square-planar geometry. Moreover, the g_{\parallel} and A_{\parallel} values of **4–6** are found in the region characteristic of CuN_2S_2 chromophores in the g_{\parallel} vs. A_{\parallel} diagram. Sakaguchi and Addison [21] showed that the $g_{\parallel}/A_{\parallel}$ ratio can be used as a convenient empirical index of tetrahedral distortion in CuN_4 units. This value ranges from ca. 105 to 135 cm for the square-planar structure, and this quotient increases on the introduction of tetrahedral distortion to the chromophore. Further, tetrahedral distortion of a square-planar chromophore is observed when any (N, O, S) donors reduce A_{\parallel} and increase g_{\parallel} . Using that relationship and the results in Table 1, compounds **4–6** present tetrahedral distortions from the square-planar geometry. The crystal structures of **4** and **5** (see Section 2.6) reveal that the geometries of these complexes are distorted square-planar or distorted tetrahedral. From the EPR data we may infer that the geometry of **6** is probably closer to the square-planar arrangement. The increased g_{\parallel} values and decreased A_{\parallel} values for the studied compounds, in the order **6**, **5**, and **4**, respectively, show that the ligand field strength decreases in these compounds in the same order [22].

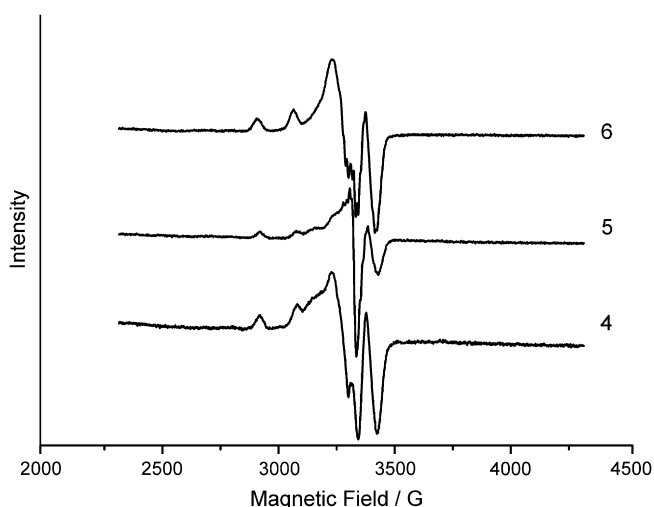


Fig. 3. X-band EPR spectra of frozen solutions of $[\text{Cu}(\text{4NO}_2\text{Ac4M})_2]$ (**4**), $[\text{Cu}(\text{4NO}_2\text{Ac4DM})_2]$ (**5**) and $[\text{Cu}(\text{4NO}_2\text{Ac4Pip})_2]$ (**6**), in DMF.

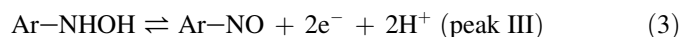
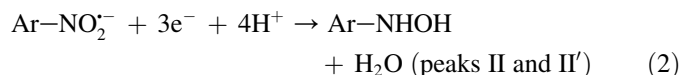
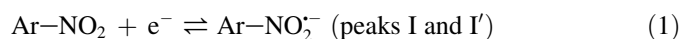
Table 1
EPR parameters g , A ($\times 10^{-4} \text{ cm}^{-1}$) and $g_{\parallel}/A_{\parallel}$ ratio for $[\text{Cu}(\text{4NO}_2\text{Ac4M})_2]$ (**4**), $[\text{Cu}(\text{4NO}_2\text{Ac4DM})_2]$ (**5**) and $[\text{Cu}(\text{4NO}_2\text{Ac4Pip})_2]$ (**6**)

Compound	g_{\parallel}	A_{\parallel}	g_{\parallel}	A_{\parallel}	$g_{\parallel}/A_{\parallel}$
4	2.0300	30	2.1530	153	141
5	2.0360	25	2.1500	158	136
6	2.0380	25	2.1365	160	133

2.5. Electrochemistry

Fig. 4 shows the voltammogram and the differential pulse voltammogram of $\text{H4NO}_2\text{Ac4M}$, and Fig. 5 shows the voltammogram of complex **4**.

The voltammograms of the thiosemicarbazones show a quasi-reversible process around -1.00 V , which has been attributed to the formation of the $\text{Ar}-\text{NO}_2^-$ radical. The second process between -1.28 and -1.48 V has been assigned to the formation of the $\text{Ar}-\text{NHOH}$ species and the irreversible oxidation at 0.08 – 0.17 V to the formation of $\text{Ar}-\text{NO}$ (see Table 2). The observed signals correspond to the well known mechanism for the nitro aromatic reduction, as proposed before in many different works [23–26]. Eqs. (1)–(3) describe the suggested electrochemical mechanism.



The voltammograms of complexes **4–6** show a quasi-reversible process attributed to the $\text{Cu}^{\text{II}}/\text{Cu}^{\text{I}}$ reduction (between -0.62 and -0.49 V) followed by the $\text{Cu}^{\text{I}}/\text{Cu}^{\text{II}}$ oxidation (between -0.43 and -0.26 V) (see Table 3). The process occurring in the

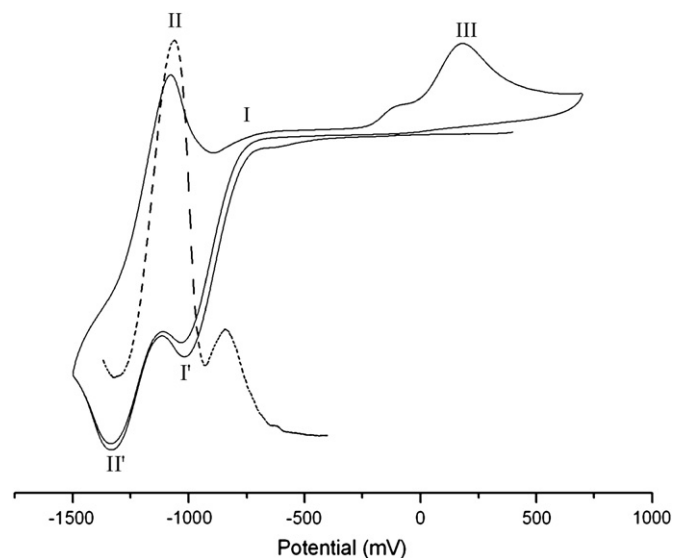


Fig. 4. Cyclic voltammogram and differential pulse voltammogram of $N(4)$ -methyl-4-nitroacetophenone thiosemicarbazone ($\text{H4NO}_2\text{Ac4M}$, **1**) (CH_2Cl_2 , 0.1 mol L^{-1} TBAP).

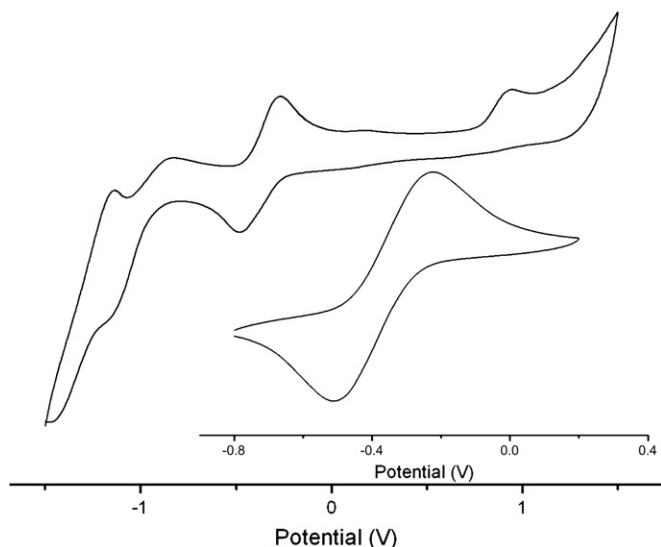


Fig. 5. Cyclic voltammogram of $[\text{Cu}(\text{4NO}_2\text{Ac4M})_2]$ (**4**) (0.100 V s^{-1} , CH_2Cl_2 , 0.1 mol L^{-1} TBAP).

–1.15 and –1.20 V range has been attributed to the formation of Ar–NHOH. The remaining processes have been assigned to the thiosemicarbazone moiety, as previously proposed by us [27]. The formation of the Ar–NO₂[•] radical has not been observed separately in the voltammograms of the complexes, indicating that in this case, once formed the radical reacts immediately.

The foregoing results show that within the nitro-aryl moiety the electrochemical behaviors of the three thiosemicarbazones are very similar, as are the behaviors of the complexes.

2.6. Crystal structures of $\text{H4NO}_2\text{4DM}$ (**2**), $[\text{Cu}(\text{4NO}_2\text{Ac4M})_2]$ (**4**) and $[\text{Cu}(\text{4NO}_2\text{Ac4DM})_2]$ (**5**)

Crystal data and refinement results of **2**, **4** and **5** are shown in Table 4. ORTEP3 views [28] of the structures can be seen in Figs. 6–8. Table 5 shows selected bond distances [Å] and angles [°] for the studied compounds.

Single crystals of **2** and complexes **4** and **5** adequate for structural X-ray diffraction work were obtained by slow evaporation of the solvent (ethanol in the case of **2** and acetone in the case of **4** and **5**).

The crystal structure of **1** has been reported previously by us [12]. Compound **2** crystallizes in the orthorhombic system, *Pcab* space group with $Z = 8$ (see Table 4 and Fig. 6). Unlike **1**, which crystallizes in the *EE* configuration in relation to C7–N2 and N3–C8, **2** adopts the *EZ* configuration.

Table 2
Cyclic voltammetry data for $\text{H4NO}_2\text{Ac4M}$ (**1**), $\text{H4NO}_2\text{Ac4DM}$ (**2**) and $\text{H4NO}_2\text{Ac4Pip}$ (**3**) (0.100 V s^{-1} , CH_2Cl_2 , 0.1 mol L^{-1} TBAP)

Compound	Ar–NO ₂ [•] (V)		Ar–NHOH (V)		Ar–NO (V)
	E_{pc}	E_{pa}	E_{pc}	E_{pa}	E_{pa}
3	–0.95	–0.96	–1.28	–1.14	0.08
1	–1.02	–0.98	–1.34	–1.09	0.17
2	–1.14	–0.99	–1.48	–1.09	0.17

Table 3
Cyclic voltammetry data for $[\text{Cu}(\text{4NO}_2\text{Ac4M})_2]$ (**4**), $[\text{Cu}(\text{4NO}_2\text{Ac4DM})_2]$ (**5**) and $[\text{Cu}(\text{H4NO}_2\text{Ac4Pip})_2]$ (**6**) (0.100 V s^{-1} , CH_2Cl_2 , 0.1 mol L^{-1} TBAP)

Compound	Cu ^{II} /Cu ^I (V)	Cu ^I /Cu ^{II} (V)	Ar–NHOH (V)
4	–0.49	–0.26	–1.15
5	–0.57	–0.35	–1.20
6	–0.62	–0.43	–1.20

The bond distances are very similar in **2** and **1**. However, O1–N1 is 1.217(5) in **2** and 1.233(4) in **1**, probably because these atoms are involved in intermolecular hydrogen bonding in the latter but not in the former compound. The N3–C8–N4, N3–C8–S and C7–N2–N3 bond angles are different in the two compounds. Steric effects could be responsible for the differences but electronic effects of two methyl groups instead of one could also have some contribution to these variations.

The crystal structure of complex **4** shows one independent molecule per asymmetric unit (see Fig. 7). One of the coordinated thiosemicarbazones presents a disorder at the terminal nitrogen N4. The difference Fourier map showed a residual electron density that could be interpreted in terms of a disordered acetone solvent molecule.

Variations in bond distances and angles were observed upon complexation of **1** (see Table 5). The C8–S bond distance changes from 1.682(3) Å in the free thiosemicarbazone to 1.749(6) Å and 1.776(7) Å in complex **4**, as a consequence of deprotonation at N3 and formation of an extensively delocalized system involving the thiosemicarbazone moiety and the aromatic ring attached to C7. Therefore the C–S bond changes from mainly double in **1** to predominantly single in **4**. The C8–N3 bond changes from 1.364(5) Å in the thiosemicarbazone to 1.313(7) Å and 1.282(8) Å in complex **4**, indicating the formation of a new predominant double bond in each ligand. The N2–N3 bond goes from 1.377(4) Å in **1** to 1.396(5) Å and 1.372(6) Å in **4**.

Compound **1** crystallizes in the *EE* configuration in relation to the C7–N2 and N3–C8 bonds, respectively. Compound **4** crystallizes in the *EZ* configuration, in which a twisting of approximately 180° in the N3–C8 bond occurs, to match the steric requirements of coordination through the N2–S system.

The angles in the thiosemicarbazone chain undergo significant changes on coordination (see Table 5). For example, the N3–C8–S angle goes from 119.7(3)° in **1** to 126.5(4)° and 126.8(5)° in **4**; the N3–N2–C7 angle changes from 119.6(3)° in **1** to 115.7(4)° and 116.0(5)° in **4** and the N2–N3–C8 angle changes from 118.3(3)° in **1** to 112.2(4)° and 111.8(5)° in **4**. Upon coordination a variation occurs in the angle between the aromatic ring and the thiosemicarbazone chain, which changes from 24.7° [12] in the free thiosemicarbazone to 40.3(1)° and 41.3(1)° in complex **4**.

Variations in some bond distances and angles also occur upon coordination of **2** with formation of complex **5** (see Table 5 and Fig. 8).

Comparison between the crystal structures of complexes **4** and **5** reveals that in both the sulfurs are approximately in *cis* position to each other. Interestingly, the crystal structure of $[\text{Ni}(\text{4NO}_2\text{Ac4M})_2]$ previously reported by us [12] shows that in this case the sulfurs are *cis* to each other as well.

Table 4
Crystal data, structure solution methods and refinement results for H4NO₂Ac4DM (**2**), [Cu(4NO₂Ac4M)₂] (**4**) and [Cu(4NO₂Ac4DM)₂] (**5**)

Compound	H4NO ₂ Ac4DM	[Cu(4NO ₂ Ac4M) ₂]·CH ₃ COCH ₃	[Cu(4NO ₂ Ac4DM) ₂]
Empirical formula	C ₁₁ H ₁₄ N ₄ O ₂ S	C ₂₃ H ₂₈ CuN ₈ O ₅ S ₂	C ₂₂ H ₂₆ CuN ₈ O ₄ S ₂
Formula weight	266.32	624.19	594.20
Temperature, K	293 (2)		
Crystal system	Orthorhombic	Orthorhombic	Monoclinic
Space group	<i>Pbca</i>	<i>Pbca</i>	<i>P21/n</i>
Unit cell dimensions			
<i>a</i> , Å	13.910(1)	13.554(1)	8.892(3)
<i>b</i> , Å	7.766(1)	15.271(1)	24.386(3)
<i>c</i> , Å	23.834(2)	27.132(3)	12.316(3)
α , °	90	90	90
β , °	90	90	92.43(2)
γ , °	90	90	90
Volume, Å ³	2574.7(4)	5615.9(8)	2668.2(12)
Z, Density calc., Mg/m ³	8, 1.374	8, 1.476	4, 1.484
Absorption coefficient, mm ⁻¹	0.252	0.975	1.020
<i>F</i> (000)	1120	2552	1236
Crystal size, mm ³	0.20 × 0.15 × 0.10	0.15 × 0.20 × 0.20	0.15 × 0.20 × 0.40
Crystal color, shape	Orange, prismatic	Dark green, prismatic	Dark red, prismatic
Rad., graph. Monoch.	Mo K α , λ = 0.71073 Å		
θ range for data coll., °	2.25–26.00	1.50–25.50	1.67–25.00
Index range, θ	0 ≤ <i>h</i> ≤ 17 -5 ≤ <i>k</i> ≤ 9 -29 ≤ <i>l</i> ≤ 0	-4 ≤ <i>h</i> ≤ 16 -1 ≤ <i>k</i> ≤ 18 -1 ≤ <i>l</i> ≤ 32	-1 ≤ <i>h</i> ≤ 10 -1 ≤ <i>k</i> ≤ 29 -14 ≤ <i>l</i> ≤ 14
Completeness	99.9% (to ϑ = 26.00°)	100% (to ϑ = 25.50°)	100% (to ϑ = 25.00°)
Refinement method	Full-matrix least-squares on <i>F</i> ²		
Goodness-of-fit on <i>F</i> ²	0.940	0.998	1.048
Reflections collected/unique (<i>R</i> _{int})	3187/2524 (0.0686)	6862/5239 (0.0415)	5451/4703 (0.0517)
Data [<i>I</i> > 2 σ (<i>I</i>)]/restraints/parameters	1346/0/163	2912/0/371	2872/0/334
<i>R</i> _{obs} , <i>R</i> _{all}	0.0600/0.1324	0.0611/0.1328	0.0675/0.1236
<i>wR</i> _{2obs} , <i>wR</i> _{2all}	0.1489/0.1916	0.1361/0.1700	0.1624/0.1933
Larg. peak and hole, e Å ⁻³	0.220 and -0.234	0.537 and -0.438	0.450 and -0.332

2.7. *In vitro* anti-trypanosomal activity

Table 6 shows the effect of the thiosemicarbazones and their corresponding copper complexes on the growth of the epimastigote form of *T. cruzi* at 25 μ M at day 5 of exposure (percentage of growth inhibition, PGI). At this dose **2** and complexes **4** and **5** proved to be as active as the reference drugs, nifurtimox (nfx) and benznidazole (bnz). Complex **6** did not inhibit *T. cruzi* growth under the assayed conditions. For the most active compounds (**2** and complexes **4** and **5**) dose–response curves were recorded and the dose that inhibits 50% of *T. cruzi* growth (ID_{50,*T. cruzi*}) was calculated (Fig. 9). The effect of copper(II) as the acetate and sulfate salts was evaluated and the low bioactivity of these salts as well as that of complex **6** indicates that copper(II) does not possess anti-*T. cruzi* activity *per se*.

2.8. *In vitro* mammal cytotoxicity

After the first screening, new *in vitro* studies were performed to analyze the nonspecific toxicity of the best anti-*T. cruzi* compounds using THP-1 human macrophages as model. The ID_{50,macrophage} values are presented in Table 6 and the therapeutic index (TI) defined as the ratio ID_{50,macrophage}/ID_{50,*T. cruzi*} is reported. Among the best anti-*T. cruzi* compounds **2** presented the highest therapeutic index.

3. Conclusion

Compound **2** proved to be the most active of the three assayed thiosemicarbazones. From the determined values of ID_{50,*T. cruzi*}, **2** as well as complexes **4** and **5** proved to be as active as the reference drugs nfx and bnz. Complex **5** exhibited high activity at very low dose (0.056 μ M). However, although it presents a good therapeutic index (TI), the therapeutic index of the free thiosemicarbazone (**2**) is higher. The therapeutic indexes (TI) of **2** and complex **5** are much higher than those of the clinically used drugs nfx and bnz, indicating that the thiosemicarbazone and the copper(II) complexes could be anti-trypanosomal drug candidates.

The significant enhancement of activity upon complexation could be due either to changes in lipophilicity, to the rigid conformation of the ligand in the complex, which could facilitate its interaction with the biological target, to a greater stability of the thiosemicarbazone in the complex or to redox effects involving the thiosemicarbazone and copper. It is clear that copper(II) *per se* is not responsible for the studied anti-*T. cruzi* activity.

As already mentioned, the mechanisms of action of nfx and bnz involve intracellular reduction of the nitro group. Nfx acts via reduction of the nitro group to an unstable nitro anion radical, which produces highly toxic reduced oxygen species (ROS) such as superoxide [8]. The mode of action of bnz involves

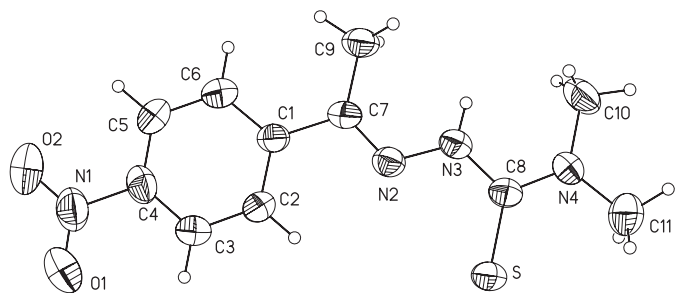


Fig. 6. Perspective view of the structure of H4NO₂Ac4DM (2).

covalent modification of biomacromolecules by nitro reduction intermediates which cause cellular damage. Similar mechanisms could be proposed for nitro thiosemicarbazones [2,29].

Our results suggest that probably the differences in activity between the three thiosemicarbazones cannot be attributable to variations in the electrochemical potentials involving the nitro group. Similarly, the different activities of the complexes are probably not due to distinct electrochemical behaviors involving the nitro-aryl moiety.

Interestingly, other authors observed a similar effect of enhancement of the anti-trypanosomal activity upon coordination to copper(II), of imidazole derivatives not containing the nitro group, which therefore cannot undergo electrochemical processes involving this group [30].

Taking into consideration the serious side effects and the poor efficacy of the clinical reference drugs, as well as the appearance of resistance during treatment, acetophenone thiosemicarbazones and their copper(II) complexes could constitute a new class of anti-trypanosomal drugs.

4. Experimental

4.1. Physical measurements

Infrared spectra were recorded on a Perkin–Elmer spectrum GX CDRH FTIR system using nujol mulls between CsI plates; partial elemental analyses were obtained with a Perkin–Elmer PE 2400 analyzer. An YSI model 31 conductivity bridge was employed for molar conductivity measurements. Electronic spectra were acquired with a Hewlett Packard

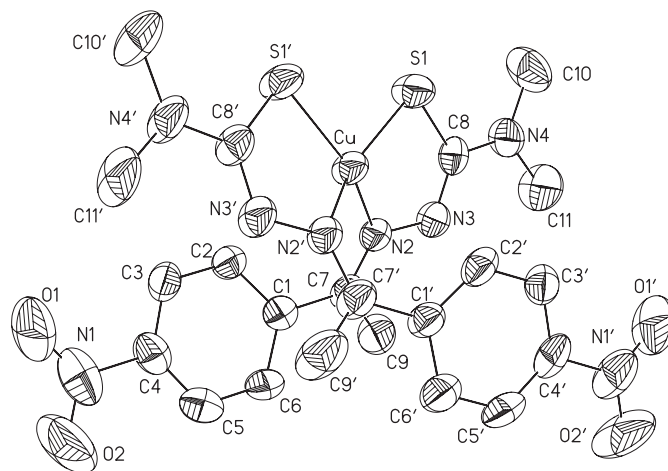


Fig. 8. Perspective view of the structure of [Cu(4NO₂Ac4DM)₂] (5).

8453 spectrometer in dimethyl formamide (DMF) solutions using 1 cm cells. NMR spectra were obtained at room temperature with a Bruker DRX-400 Avance (400 MHz) spectrometer using deuterated dimethyl sulfoxide (DMSO-*d*₆) as the solvent and tetramethylsilane (TMS) as internal reference. Splitting patterns are designated as follows; s, singlet; d, doublet; t, triplet; q, quartet; m, multiplet.

The electrochemical experiments were carried out at room temperature in dichloromethane containing 0.1 mol L⁻¹ tetrabutylammonium perchlorate (TBAP) purchased from Fluka. These measurements were performed by using an electrochemical analyzer from Bioanalytical Systems Inc. (BAS), model 100BW. The working and auxiliary electrodes were stationary Pt foils, and the reference electrode was Ag/AgCl a medium in which ferrocene is oxidized at 0.48 V (Fc⁺/Fc).

EPR spectra of the copper(II) complexes were obtained at 77 K (liquid N₂ temperature) on a VARIAN E109-110 equipment operating at about 9.5 GHz (X-band) using DMF as solvent.

4.2. X-ray crystallography

The crystal structures of H4NO₂4DM (2), [Cu(4NO₂Ac4M)₂] (4), and [Cu(4NO₂Ac4DM)₂] (5) were investigated using a SIEMENS P4 diffractometer at 273 K with a graphite monochromator and Mo K α radiation $\lambda = 0.71073$ Å. Data were obtained using the XSCANS software [31]. The lattice parameters were obtained by least-squares fit from 21/43/42 accurately centered reflections in the 2θ range 8.5–12.2/5.3–12.5/8.5–10.4 for H4NO₂4DM (2), [Cu(4NO₂Ac4M)₂] (4), and [Cu(4NO₂Ac4DM)₂] (5), respectively. Data were corrected for Lorentz and polarization effects, but not for absorption. The structures were solved by direct methods and refined by full-matrix-least-squares on F^2 using SHELX97 [32]. Although some of the hydrogen atoms could be identified in a Fourier difference map, in the final model they were geometrically positioned and refined using a riding model. All non-H atoms were refined anisotropically.

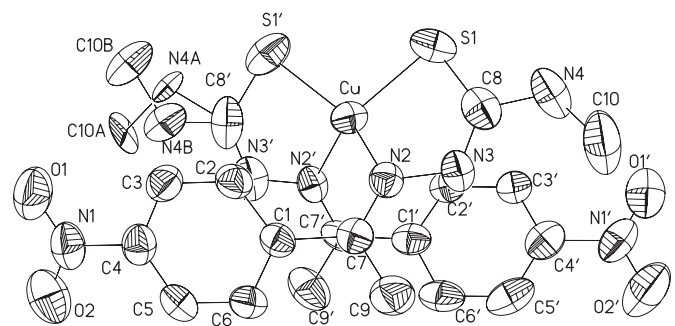


Fig. 7. Perspective view of the structure of [Cu(4NO₂Ac4M)₂] (4).

Table 5

Selected bond lengths [Å] and angles [°] for H4NO₂Ac4DM (2), [Cu(4NO₂Ac4M)₂] (4) and [Cu(4NO₂Ac4DM)₂] (5)

Bond	2 [Å]	4 [Å]	4 [Å]	5 [Å]	5 [Å]	Angle	2 [°]	4 [°]	4 [°]	5 [°]	5 [°]
		Ligand 1	Ligand 2	Ligand 1	Ligand 2		Ligand 1	Ligand 2	Ligand 1	Ligand 2	Ligand 1
S–C8	1.680(4)	1.749(6)	1.776(7)	1.750(6)	1.735(6)	C8–N4–C10	122.7(4)	123.5(5)	–	123.8(6)	123.1(6)
C8–N3	1.372(5)	1.313(7)	1.282(8)	1.318(7)	1.307(7)	N4–C8–S	123.5(3)	116.9(5)	–	117.8(5)	117.6(5)
C8–N4	1.340(5)	1.351(7)	–	1.347(7)	1.355(7)	N4–C8–N3	114.0(3)	116.6(5)	–	117.6(5)	117.0(5)
N3–N2	1.374(4)	1.396(5)	1.372(6)	1.379(6)	1.403(6)	N3–C8–S	122.5(3)	126.5(4)	126.8(5)	124.6(4)	125.3(4)
C7–N2	1.284(5)	1.288(6)	1.294(6)	1.287(7)	1.288(7)	N2–N3–C8	120.1(3)	112.2(4)	111.8(5)	113.3(4)	113.3(5)
N1–O1	1.217(5)	1.223(6)	1.212(7)	1.215(9)	1.236(9)	C7–N2–N3	117.2(3)	115.7(4)	116.0(5)	114.7(4)	114.5(5)
N1–O2	1.214(5)	1.211(6)	1.207(6)	1.219(9)	1.192(9)	N2–Cu–N2'	–	100.5(2)	–	105.1(2)	–
Cu–N2	–	2.018(4)	2.007(4)	2.027(5)	2.018(5)	N2'–Cu–S'	–	84.6(1)	–	84.9(1)	–
Cu–S	–	2.238(2)	2.232(2)	2.226(2)	2.224(2)	N2–Cu–S	–	85.2(1)	–	84.5(1)	–
						N2–Cu–S'	–	148.0(1)	–	156.4(2)	–
						N2'–Cu–S	–	150.9(1)	–	155.7(2)	–
						S–Cu–S'	–	105.7(1)	–	95.0(1)	–

': Atom of the second ligand.

4.3. Synthesis of H4NO₂Ac4M (1), H4NO₂Ac4DM (2) and H4NO₂Ac4Pip(3)

N(4)-Methyl thiosemicarbazide was purchased from Aldrich and used without further purification. N(4)-Dimethyl and N(4)-piperidyl thiosemicarbazides were prepared as previously reported [33]. The thiosemicarbazones were obtained by mixing equimolar amounts of 4-nitroacetophenone (6.6×10^{-3} mol) with the desired N(4)-substituted thiosemicarbazide in absolute ethanol (40 mL) with addition of 2–4 drops of concentrated sulfuric acid as catalyst. The reaction mixture was kept under reflux for 6–7 h. The resulting solids were filtered off and re-crystallized from ethanol.

4.3.1. N(4)-Methyl 4-nitroacetophenone thiosemicarbazone (H4NO₂Ac4M, 1)

N(4)-Methyl 4-nitroacetophenone thiosemicarbazone (H4NO₂Ac4M, 1) has been reported previously [12].

4.3.2. N(4)-Dimethyl 4-nitroacetophenone thiosemicarbazone (H4NO₂Ac4DM, 2)

Orange solid; yield: 77%; mp: 182.0–183.0 °C. Anal. Calcd (C₁₁H₁₄N₄O₂S): C, 49.61; H, 5.30; N, 21.04. Found: C, 49.16; H, 5.35; N, 21.02%. UV: λ_{\max} (cm⁻¹): 36,900, 27,951. IR (nujol mulls, cm⁻¹): $\nu_{\text{ass-NO}_2}$ 1535, $\nu_{\text{s-NO}_2}$ 1329, $\nu(\text{NH})$ 3330, $\nu(\text{C}=\text{N})$ 1590, $\nu(\text{C}=\text{S})$ 809. ¹H NMR (DMSO-*d*₆): (δ , ppm) 9.76 (1H, s, N(3)H), 8.29 (2H, d, aryl H(3,5), *J* = 8.93), 8.05 (2H, d, aryl H(2,6), *J* = 8.93), 3.32 (6H, s, H(10,11)), 2.35 (3H, s, H(9)), C8=S 182.08, C4 147.43, C1 147.31, C7=N 144.31, C2 and C6 127.08, C3 and C5 123.56, C10 and C14 42.20, C9 13.78.

4.3.3. N(4)-Piperidyl 4-nitroacetophenone thiosemicarbazone (H4NO₂Ac4Pip, 3)

Yellow solid; yield: 72%; mp: 144.9–146.0 °C. Anal. Calcd (C₁₄H₁₈N₄O₂S): C, 54.88; H, 5.92; N, 18.29. Found: C, 54.05; H, 5.83; N, 18.72%. UV: λ_{\max} (cm⁻¹): 36,900,

Table 6

In vitro anti-*T. cruzi* activities and human macrophages cytotoxicities for H4NO₂Ac4M (1), H4NO₂Ac4DM (2), H4NO₂Ac4Pip (3) and their copper(II) complexes [Cu(4NO₂Ac4M)₂] (4) and [Cu(4NO₂Ac4DM)₂] (5) and [Cu(4NO₂Ac4Pip)₂] (6)

Thiosemicarbazones					Copper complexes				
Compound	PGI ^a (%)	ID _{50,<i>T. cruzi</i>} ^{b,c} (μM)	ID _{50,macrophage} ^{c,d} (μM)	TI ^e	Compound	PGI ^a (%)	ID _{50,<i>T. cruzi</i>} ^{b,c} (μM)	ID _{50,macrophage} ^{c,d} (μM)	TI ^e
1	31	>25.0	>400.0	>16	4	100	2.0	4.0	2
2	100	0.28	>400.0	>1428	5	100	0.056	50.0	893
3	12	>>25.0	ND ^f	ND	6	0	>>25.0	ND	ND
Nfx	100	7.7	>300.0 ^g	>38	Copper(II) acetate ^g	>>2.0 ^h			
Bnz	100	7.4	>300.0 ^g	>40	Copper(II) sulfate ^g	>>2.0 ⁱ			

^a PGI: percentage of growth inhibition at 25 μM , epimastigote form of *T. cruzi* Tulahuen 2.^b ID_{50,*T. cruzi*}: dose that inhibits 50% of *T. cruzi* growth.^c The results are the mean values of three different experiments with a SD less than 10% in all cases.^d ID_{50,macrophage}: dose that inhibits 50% of THP-1 human macrophages growth.^e TI: therapeutic index, see text for definition.^f ND: not determined.^g The following doses were studied: 2.0, 1.0, 0.5 and 0.1 μM .^h The salt resulted inactive in the 0.1–1.0 μM range; PGI at 2.0 μM = 15%.ⁱ The salt resulted inactive in the 0.1–1.0 μM range; PGI at 2.0 μM = 5%.^j Higher doses were not assayed due to solubility problems.

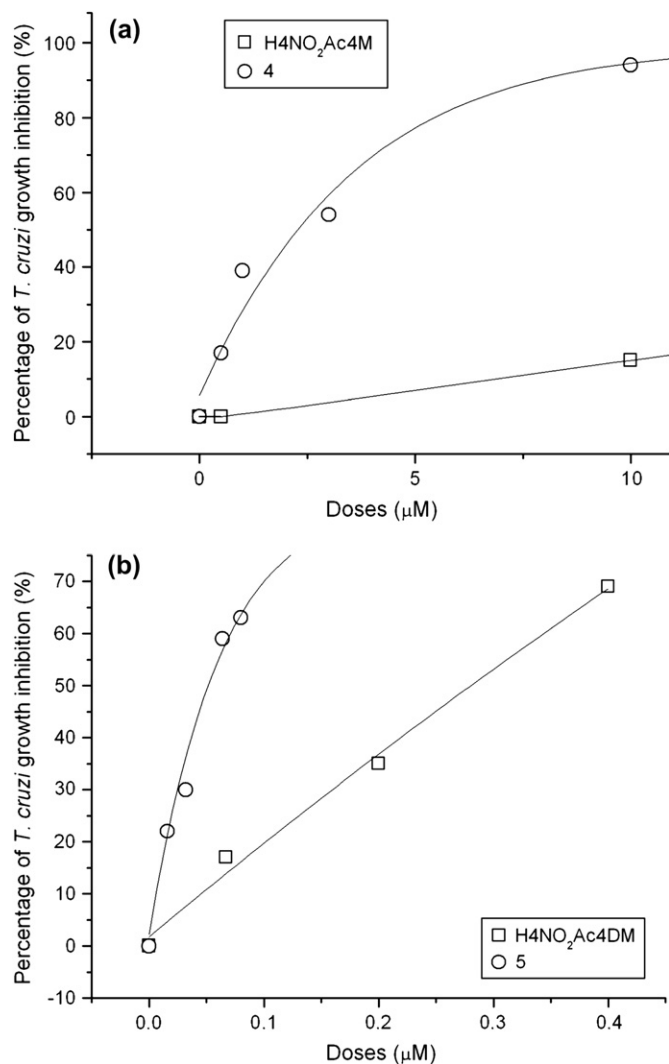


Fig. 9. Curves dose–anti-*T. cruzi* activity for (a) H4NO₂Ac4M and complex (4); (b) H4NO₂Ac4DM and complex (5).

27,225. IR (nujol mulls, cm^{-1}): ν_{assNO_2} 1538, ν_{sNO_2} 1332, $\nu(\text{C}=\text{N})$ 1590, $\nu(\text{C}=\text{S})$ 806. NMR (DMSO-*d*₆): (δ , ppm) 9.84 (1H, s, N(3)H), 8.25 (2H, d, aryl H(3,5), $J = 8.97$), 8.01 (2H, d, aryl H(2,6), $J = 8.97$), 3.87 (4H, s, H(10,14)), 2.35 (3H, s, H(9)), 1.65 (6H, s, H(11,12,13)), C8=S 182.00, C4 147.27, C1 146.81, C7=N 144.22, C2 and C6 127.03, C3 and C5 123.56, C10 and C14 51.46, C11 and C13 25.78, C12 23.87, C9 13.94.

4.4. Synthesis of [Cu(4NO₂Ac4M)₂] (4), [Cu(4NO₂Ac4DM)₂] (5) and [Cu(4NO₂Ac4Pip)₂] (6)

The copper(II) complexes were obtained by reacting the desired thiosemicarbazone (0.002 mol) in methanol (30 mL) with copper(II) acetate (0.001 mol) in 30 mL of methanol. The reaction mixture was kept at 3 °C under stirring while the thiosemicarbazones were added. The resulting solids were filtered, washed with anhydrous diethyl ether and re-crystallized from ethanol.

4.4.1. [Cu(4NO₂Ac4M)₂] (4)

Green solid; yield: 83%. Anal. Calcd (C₂₀H₂₂CuN₈O₄S₂): C, 42.43; H, 3.92; N, 19.79. Found: C, 42.06; H, 3.84; N, 19.66%. UV: λ_{max} (cm^{-1}): 29,939, 25,060, 16,664. IR (nujol mulls, cm^{-1}): ν_{assNO_2} 1521, ν_{sNO_2} 1340, $\nu(\text{NH})$ 3438, $\nu(\text{C}=\text{N})$ 1568, $\nu(\text{C}=\text{S})$ 751, $\nu(\text{M}-\text{N})$ 432, $\nu(\text{M}-\text{S})$ 350. Molar conductivity (1×10^{-3} mol L⁻¹ DMF): $1.44 \Omega^{-1} \text{cm}^2 \text{mol}^{-1}$. Magnetic susceptibility: 1.50μ (BM).

4.4.2. [Cu(4NO₂Ac4DM)₂] (5)

Brown solid; yield: 82%. Anal. Calcd (C₂₂H₂₆CuN₈O₄S₂): C, 44.47; H, 4.41; N, 18.86. Found: C, 43.81; H, 4.40; N, 18.72%. UV: λ_{max} (cm^{-1}): 29,939, 24,413, 16,820. IR (nujol mulls, cm^{-1}): ν_{sNO_2} 1331, $\nu(\text{C}=\text{N})$ 1572, $\nu(\text{C}=\text{S})$ 725, $\nu(\text{M}-\text{N})$ 448, $\nu(\text{M}-\text{S})$ 322. Molar conductivity (1×10^{-3} mol L⁻¹ DMF): $2.00 \Omega^{-1} \text{cm}^2 \text{mol}^{-1}$. Magnetic susceptibility: 1.80μ (BM).

4.4.3. [Cu(4NO₂Ac4Pip)₂] (6)

Yellowish green solid; yield: 78%. Anal. Calcd (C₂₈H₃₄CuN₈O₄S₂): C, 49.87; H, 5.08; N, 16.62. Found: C, 48.09; H, 5.04; N, 16.50%. UV–vis (cm^{-1}): 29,561, 24,312, 17,126. IR (nujol mulls, cm^{-1}): ν_{sNO_2} 1330, $\nu(\text{C}=\text{N})$ 1585, $\nu(\text{C}=\text{S})$ 719, $\nu(\text{M}-\text{N})$ 452, $\nu(\text{M}-\text{S})$ 368. Molar conductivity (1×10^{-3} mol L⁻¹ DMF): $7.21 \Omega^{-1} \text{cm}^2 \text{mol}^{-1}$. Magnetic susceptibility: 1.80μ (BM).

4.5. In vitro anti-trypanosomal activity

T. cruzi epimastigotes (Tulahuen 2 strain) were grown at 28 °C in an axenic medium (BHI-Tryptose) as previously described [2,6–8], complemented with 5% fetal calf serum. Cells were harvested in the late log phase, re-suspended in fresh medium, counted in Neubauer's chamber and placed in 24-well plates ($2 \times 10^6/\text{mL}$). Cell growth was measured as the absorbance of the culture at 590 nm, which was proved to be proportional to the number of cells present [34]. Before inoculation, the media were supplemented with the indicated amount of the studied compound from a stock solution in DMSO. The final concentration of DMSO in the culture media never exceeded 1% and the control was run in the presence of 1% DMSO and in the absence of any compound. No effect on epimastigotes growth was observed by the presence of up to 1% DMSO in the culture media. Nfx and bnz were used as the reference trypanocidal drugs. Copper(II) acetate and copper(II) sulfate were included in these assays to provide information on the trypanocidal effect of copper, as copper(II) entity. The percentage of growth inhibition (PGI), was calculated as follows: $\text{PGI} = \{1 - [(A_p - A_{0p}) / (A_c - A_{0c})]\} \times 100$, where $A_p = A_{600}$ of the culture containing the studied compound at day 5; $A_{0p} = A_{600}$ of the culture containing the studied compound right after addition of the inocula (day 0); $A_c = A_{600}$ of the culture in the absence of any compound (control) at day 5; $A_{0c} = A_{600}$ in the absence of the compound at day 0. To determine ID_{50,T. cruzi} values, parasite growth was followed in the absence (control) and presence of increasing concentrations of the corresponding compound. The ID_{50,T.}

cruzi values were determined as the drug concentrations required to reduce by half the absorbance of that of the control (without compound).

4.6. In vitro cytotoxicity to macrophages

THP-1 human macrophages were seeded (100.000 cells/well) in 96-well flat bottom microplates (Nunc) with 200 μ L of RPMI 1640 medium supplemented with 20% heat inactivated fetal calf serum. Cells were allowed to attach for 24 h in a humidified 5% CO₂/95% air atmosphere at 37 °C. Then, cells were exposed to the compounds (1–400 μ M) for 48 h. Afterwards, the cells were washed with PBS and incubated (37 °C) with MTT 0.4 mg/mL for 3 h. Then, formazan was dissolved with DMSO (180 μ L) and optical densities were measured. Each concentration was assayed three times and six growth controls were used in each test. Cytotoxicity percentages (% C) were determined as follows: % C = [100 – (ODd – ODdm)/(ODc – ODcm)] \times 100, where ODd is the mean of OD₅₉₅ of wells with macrophages and different concentrations of the compounds; ODdm is the mean of OD₅₉₅ of wells with different compound concentrations in the medium; ODc is the growth control and ODcm is the mean of OD₅₉₅ of wells with only medium. The ID_{50,macrophage} values were determined as the drug concentrations required to reduce by half the absorbance of that of the control (without compound) [35].

5. Supplementary material available

Crystallographic data for compound H4NO₂Ac4DM (**2**), [Cu(4NO₂Ac4M)₂] (**4**) and [Cu(4NO₂Ac4DM)₂] (**5**) have been deposited at Cambridge Crystallographic Data Centre as supplementary publication numbers CCDC 626173, CCDC 626172, and CCDC 626171, respectively. Copies of available material can be obtained on application to CCDC, 12 Union Road, Cambridge CB2 1Ez, UK (fax: +44 1223 336 033 or e-mail: deposit@ccdc.cam.ac.uk).

Acknowledgements

Financial support from Capes, CNPq-PROSUL and Fapesp from Brazil is acknowledged.

References

- [1] C. Urquiola, M. Vieites, G. Aguirre, A. Marín, B. Solano, G. Arrambide, P. Noblia, M.L. Lavaggi, M.H. Torre, M. González, A. Monge, D. Gambino, H. Cerecetto, *Bioorg. Med. Chem.* 14 (2006) 5503–5509.
- [2] G. Aguirre, L. Boiani, H. Cerecetto, M. Fernández, M. González, A. Denicola, L. Otero, D. Gambino, C. Rigol, C. Olea-Azar, M. Faundez, *Bioorg. Med. Chem.* 12 (2004) 4885–4893.
- [3] (a) S.N.J. Moreno, R.P. Mason, R. Docampo, *J. Biol. Chem.* 259 (1984) 6298–6305; (b) S.N.J. Moreno, R. Docampo, R.P. Mason, W. León, A.O.M. Stoppani, *Arch. Biochem. Biophys.* 218 (1982) 585–591; (c) R. Docampo, S.N.J. Moreno, A.O.M. Stoppani, W. León, F.S. Cruz, F. Villalta, R.F. Muniz, *Biochem. Pharmacol.* 30 (1981) 1947–1951.
- [4] H. Beraldo, D. Gambino, *Mini. Rev. Med. Chem.* 4 (2004) 31–39.
- [5] H. Cerecetto, R. Di Maio, G. Ibarruri, G. Seoane, A. Denicola, G. Peluffo, C. Quijano, M. Paulino, *Il Farmaco* 53 (1998) 89–94.
- [6] H. Cerecetto, R. Di Maio, M. González, M. Risso, G. Sagraera, G. Seoane, A. Denicola, G. Peluffo, C. Quijano, A.O.M. Stoppani, M. Paulino, C. Olea-Azar, M.A. Basombrío, *Eur. J. Med. Chem.* 35 (2000) 343–350.
- [7] L. Otero, P. Noblia, D. Gambino, H. Cerecetto, M. González, J.A. Ellena, O.E. Piro, *Inorg. Chim. Acta* 344 (2003) 85–94 and references therein.
- [8] L. Otero, M. Vieites, L. Boiani, A. Denicola, C. Rigol, L. Opazo, C. Olea-Azar, J.D. Maya, A. Morello, R.L. Krauth-Siegel, O.E. Piro, E. Castellano, M. González, D. Gambino, H. Cerecetto, *J. Med. Chem.* 49 (2006) 3322–3331.
- [9] R.A. Sánchez-Delgado, A. Anzellotti, L. Suárez, in: H. Sigel, A. Sigel (Eds.), *Metal Ions in Biological Systems*, vol. 41, Marcel Dekker, New York, 2004, pp. 379–419.
- [10] (a) F. Arjmand, B. Mohani, S. Ahmad, *Eur. J. Med. Chem.* 40 (2005) 1103–1110; (b) N.K. Singh, S.B. Singh, *Met. Based Drugs* 9 (2002) 109–118; (c) D. Jayaraju, A.K. Kondapi, *Curr. Sci.* 81 (2001) 787–792.
- [11] (a) N.V. Loginova, T.V. Koval'chuk, R.A. Zheldakova, N.P. Osipovich, V.L. Sorokin, G.I. Polozov, G.A. Ksendzova, G.K. Glushonok, A.A. Chernyavskaya, O.I. Shadyro, *Bioorg. Med. Chem. Lett.* 16 (2006) 5403–5407; (b) S. Sharma, F. Athar, M.R. Maurya, A. Azam, *Eur. J. Med. Chem.* 40 (2005) 1414–1419; (c) S. Sharma, F. Athar, M.R. Maurya, F. Naqvi, A. Azam, *Eur. J. Med. Chem.* 40 (2005) 557–562; (d) B. Bottari, R. Maccari, F. Monforte, R. Ottaná, E. Rotondo, M.G. Vigorita, *Bioorg. Med. Chem. Lett.* 10 (2000) 657–660; (e) J. Patole, U. Sandbhor, S. Padhye, D.N. Deobagkar, C.E. Anson, A. Powell, *Bioorg. Med. Chem. Lett.* 13 (2003) 51–55.
- [12] A. Pérez-Rebolledo, I.C. Mendes, N.L. Speziali, P. Bertani, J.M. Resende, A.F.C. Alcântara, H. Beraldo, *Polyhedron* 26 (2007) 1449–1458.
- [13] (a) I.C. Mendes, L.R. Teixeira, R. Lima, H. Beraldo, N.L. Speziali, D.X. West, *J. Mol. Struct.* 559 (2001) 355–360; (b) H. Beraldo, R. Lima, L.R. Teixeira, A.A. Moura, D.X. West, *J. Mol. Struct.* 559 (2001) 99–106.
- [14] H. Beraldo, W.F. Nacif, L.R. Teixeira, J.S. Rebouças, *Transition Met. Chem.* 27 (2002) 85–88.
- [15] I.C. Mendes, L.R. Teixeira, R.L. Lima, T.G. Carneiro, H. Beraldo, *Transition Met. Chem.* 24 (1999) 655–658.
- [16] A.P. Rebolledo, G.M. de Lima, L.N. Gambi, N.L. Speziali, D.F. Maia, C.B. Pinheiro, J.D. Ardisson, M.E. Cortés, H. Beraldo, *Appl. Organomet. Chem.* 17 (2003) 945–951.
- [17] A. Pérez-Rebolledo, M. Vieites, D. Gambino, O.E. Piro, E.E. Castellano, C.L. Zani, E.M. Souza-Fagundes, L.R. Teixeira, A.A. Batista, H. Beraldo, *J. Inorg. Biochem.* 99 (2005) 698–706.
- [18] R.L. Lima, L.R. Teixeira, T.M. Carneiro, H. Beraldo, *J. Braz. Chem. Soc.* 10 (1999) 184–188.
- [19] D.X. West, H. Beraldo, A.A. Nassar, F.A. El-Saied, M.I. Ayad, *Transition Met. Chem.* 24 (1999) 421–424.
- [20] E. Bermejo, A. Castiñeras, M. Gil, E. Labisbal, A. Sousa, H. Beraldo, D.X. West, *Z. Anorg. Allg. Chem.* 627 (2001) 827–835.
- [21] U. Sakaguchi, A.W. Addison, *J. Chem. Soc., Dalton Trans.* (1979) 600–608.
- [22] S.M. de M. Romanowski, F. Tormena, V.A. dos Santos, M.F. Hermann, A.S. Mangrich, *J. Braz. Chem. Soc.* 15 (2004) 897–903.
- [23] S. Bollo, L.J. Nuñez-Vergara, M. Bonta, G. Chauviere, J. Perie, J.A. Squella, *J. Electroanal. Chem.* 511 (2001) 46–54.
- [24] J.C.M. Cavalcanti, N.V. Oliveira, M.A.B.F. de Moura, R. Fruttero, M. Bertinaria, M.O.F. Goulart, *J. Electroanal. Chem.* 571 (2004) 177–182.
- [25] P.C. Mandal, *J. Electroanal. Chem.* 570 (2004) 55–61.
- [26] S. Bollo, L.J. Nuñez-Vergara, J.A. Squella, *J. Electroanal. Chem.* 562 (2004) 9–14.
- [27] R.F.F. Costa, A.P. Rebolledo, T. Matencio, H.D.R. Callado, J.D. Ardisson, M.E. Cortés, B.L. Rodrigues, H. Beraldo, *J. Coord. Chem.* 58 (2005) 1307–1319.

- [28] C.K. Johnson, ORTEP 11, Report ORNL-5135, Oak ridge National Laboratory, TN, 1976.
- [29] C. Rigol, C. Olea-Azar, F. Mendizábal, L. Otero, D. Gambino, M. Gonzalez, H. Cerecetto, *Spectrochim. Acta, Part A* 61 (2005) 2933–2938.
- [30] M. Navarro, E.J. Cisneros-Fajardo, T. Lehmann, R.A. Sánchez-Delgado, R. Atencio, P. Silva, R. Lira, J.A. Urbina, *Inorg. Chem.* 40 (2001) 6879–6884.
- [31] Siemens XSCANS Users Manual, Siemens Analytical X-ray Instruments, Madison, WI, 1994.
- [32] G.M. Sheldrick, SHELX97, Program for the Refinement of Crystal Structures, University of Göttingen, Germany, 1997.
- [33] D.X. West, M.M. Salberg, G.A. Bain, A.F. Liberta, *Transition Met. Chem.* 22 (1997) 180–184.
- [34] A. Denicola, H. Rubbo, D. Rodríguez, R. Radi, *Arch. Biochem. Biophys.* 304 (1993) 279–286.
- [35] S. Muelas, R. Di Maio, H. Cerecetto, G. Seoane, C. Ochoa, J.A. Escario, A. Gómez-Barrio, *Folia Parasitol.* 48 (2001) 105–108.